Theory of tunneling spectroscopy for chiral topological superconductors

Akihiro Ii, Ai Yamakage, Keiji Yada, Masatoshi Sato, and Yukio Tanaka

Theory of tunneling spectroscopy for chiral topological superconductors

Akihiro Ii,[1] Ai Yamakage,[1] Keiji Yada,[1] Masatoshi Sato,[2] and Yukio Tanaka[1]

[1]*Department of Applied Physics, Nagoya University, Nagoya 464-8603, Japan*
[2]*Institute for Solid State Physics, University of Tokyo, Chiba 277-8581, Japan*

(Dated: October 8, 2012)

We study the charge conductance of an interface between a normal metal and a superconducting quantum anomalous Hall system, based on the recursive Green's function. The angle resolved conductance $\gamma(k_y, eV)$ with the momentum k_y parallel to the interface and the bias voltage V shows a rich structure depending on the Chern number $\mathcal{N}$ of the system. We find that when the bias voltage is tuned to the energy dispersion of the edge mode, $eV = E_{\text{edge}}(k_y)$, the angle resolved conductance $\gamma(k_y, E_{\text{edge}}(k_y))$ shows a pronounced even-odd effect; the conductance vanishes for $\mathcal{N} = 0$ or 2 while it takes a universal value $2e^2/h$ for $\mathcal{N} = 1$. In particular, in $\mathcal{N} = 2$ phase, we find that the conductance $\gamma(k_y, E_{\text{edge}}(k_y))$ becomes zero due to interference of two degenerate Majorana edge modes, although the corresponding surface spectral weight remains non-zero.

I. INTRODUCTION

It is well known that Andreev bound states (ABSs) are generated at the edge of unconventional superconductors where the pair potentials change sign on their Fermi surfaces.[1–8] Nowadays, the ABSs in unconventional superconductors have been recognized as important topological objects in condensed matter physics. Superconductors hosting topologically protected ABSs are dubbed as topological superconductor,[9–12] and they are characterized by discrete symmetries such as the particle-hole symmetry.[13,14] Furthermore, it has been clarified as the bulk/edge correspondence that when a gapless ABS is generated on the edge, the corresponding topological invariant exists in the bulk system.[14–16]

For quasi-two dimensional superconductors, according to the energy dispersions, ABSs are classified into three; flat-type, chiral-type and helical type. A flat-type ABS is protected by a one-dimensional winding number which is defined for a fixed k_y, where k_y is the momentum parallel to the surface.[17,18] This flat type ABS is dubbed as mid gap Andreev bound state and is generated for nodal superconductors like spin-singlet d_{xy}-wave one or spin-triplet p_x-wave one. A chiral-type ABS has a linear energy dispersion[19–22] and is realized in spin-triplet chiral p-wave superconductors like Sr_2RuO_4.[23,24] This ABS is protected by the Chern number[9,22,25,26] and it causes a spontaneous current along the surface. A chiral ABS has been recognized as a chiral Majorana edge mode if the spin degree of freedom is quenched.[9]

By contrast to the case of chiral ABSs, the time reversal symmetry is preserved in helical ABSs. A helical ABS supports two linear energy dispersions with opposite velocities, which form a Kramers pair. Instead of a charge current, a spin current is spontaneously generated along the edge. Stability of the helical ABS is guaranteed by the $\mathbb{Z}_2$ topological invariant, as in the case of quantum spin Hall insulators (QSHs),[27], and they are expected to be realized in non-centrosymmetric superconductors[28–32] and a bilayer Rashba system,[33] where the spin-orbit coupling is important. Several new features of helical ABSs have been predicted.[34–44] Surface ABSs in three dimensional systems have been also studied. A cone-type ABS is predicted for a superconducting analogue of the superfluid ^{3}He B phase. This ABS is interpreted as Majorana fermion[9,45–48] obeying massless two dimensional Dirac equation. Moreover, surface ABSs with various complicated energy dispersions[49] appear in superconducting topological insulators,[50] e.g., $Cu_xBi_2Se_3$[51,52].

A new direction for realization of Majorana fermions is to fabricate topological superconductors with conventional pairing.[53] Especially, much attention has been paid to realize chiral Majorana modes from the view point of topological quantum computing.[54–56] There are several proposals to fabricate Majorana fermions in systems coupled to superconductor via the proximity effect. It has been proposed that a chiral Majorana edge mode is produced at the interface of ferromagnet/spin-singlet s-wave superconductor junction on the substrate of three-dimensional topological insulator.[57–62] Also, a simpler scheme using the Rashba spin-orbit interaction and the Zeeman field has been proposed.[63–69] The essential point is the simultaneous presence of the strong spin-orbit coupling and the time reversal symmetry breaking by the Zeeman field. There is another way to realize chiral Majorana edge modes by using chiral edge states of a quantum anomalous Hall system (QAH).[70] A QAH can be realized by doping of magnetic impurity in a QHS.[71] In this scheme, the presence of the chiral Majorana edge modes can be controlled by the band mass m, chemical potential μ and the pair potential Δ. The number of chiral Majorana edge modes can be classified by the Chern number $\mathcal{N}$ of the system.[9]

Stimulated by the idea of Qi et al,[70] in our previous paper, we have calculated the energy spectrum of the edge states and the resulting surface local density of states (SLDOS) for various values of the Chern number $\mathcal{N}$ in a heterostructure of a QAH and a spin-singlet s-wave superconductor (QAH+s).[72] To clarify the difference between the $\mathcal{N}=1$ and $\mathcal{N}=2$ states, we applied Zeeman magnetic fields. We have found that when the direction of the magnetic field is parallel to the interface, the degeneracy of the two chiral Majorana edge modes in $\mathcal{N}=2$ states is lifted. We have also clarified that the degeneracy is lifted by shifting the chemical potential from zero. Although the SLDOS has been calculated in detail, the relevance to the actual tunneling conductance observed in QAH+s system have not been clarified yet.

The purpose of this work is to present a theory of the tunneling conductance in this system. If the ABS has a flat dispersion, which is realized in high-T_c cuprate, the tunneling conductance is expressed by the SLDOS.[73,74] In the present case, however, the correspondence is not clear. Since the ABS has a linear dispersion, the SLDOS does not always coincide with the tunneling conductance in normal metal (N)/superconductor junction even in the low transparent limit.[38,39,75–77] A similar situation occurs in three dimensions. Differently from the case of the superconducting analogue of ^{3}He B phase,[78] the tunneling conductance for the junction of N/superconducting topological insulator shows a single zero-bias peak by taking into account a finite temperature effect[79] or transmissivity at the interface, even though the SLDOS has a double peak structure.[80] Because of the difficulty to predict the charge transport property from the SLDOS, as mentioned above, we have to calculate the tunneling conductance of N/(QAH+s)/N junction by explicitly solving the Bogoliubov-de Gennes (BdG) equation.

The organization of the paper is as follows. In Sec. II, we review the model of QAH with spin-singlet s-wave superconductor. In addition, we formulate the tunneling conductance in N/(QAH+s)/N junction using the recursive

Green's function. In Sec. III, we calculate the energy dispersion, the SLDOS and the tunneling conductances in N/QAH/N junction and N/(QAH+s)/N one. We reveal that an even-odd effect in the angle-resolved conductance occurs due to interference of Majorana fermions whereas the corresponding SLDOS does not. In Sec. IV, we summarize our results.

II. FORMULATION

In this section we show the model Hamiltonian of QAH+s and the method of numerical calculation for the SLDOS. The model of N/(QAH+s)/N junction and the formula of the tunneling conductance with the recursive Green's function are also shown.

A. Hamiltonian of QAH+s

We consider a QAH on the two-dimensional square lattice, which is obtained by the replacement $k_{x,y} \to \sin k_{x,y}$ and $k_x^2 + k_y^2 \to 4 - 2(\cos k_x + \cos k_y)$ in the model used in Refs.[70,81] Near the Γ point, this replacement does not change the low energy and low wavelength physics of the system. Compared to the continuum model, the square lattice model is convenient when we calculate the SLDOS. In the momentum space, the Hamiltonian has the form as $\mathcal{H}_{\mathrm{QAH}}(\boldsymbol{k}) = \boldsymbol{d}(\boldsymbol{k}) \cdot \boldsymbol{s}$ with

$$\boldsymbol{d}(\boldsymbol{k}) = (A \sin k_x, A \sin k_y, m(\boldsymbol{k})), \tag{1}$$

where s_i is Pauli matrix in spin space and $m(\boldsymbol{k}) = m + 2B(2 - \cos k_x - \cos k_y)$. The band mass term $m(\boldsymbol{k})$ determines the magnitude of the energy shift between up and down spins. A, B and m are material parameters corresponding to the velocity of the surface Dirac fermion, the inverse effective mass of conduction/valence bands, and the band gap, respectively. The sign of m/B determines the topological property of the system. Here note that the presence of B term is crucial to exhibit a QAH. The energy dispersion of the above Hamiltonian is symmetric with respect to the mass term m for $B = 0$, but is asymmetric for $B \neq 0$. In other words, a nonzero value of B makes the sign of m meaningful. Hereafter, we take $A = B = 1$ and the lattice constant being unity in our calculations.

In the following, we consider the proximity effect by an attached spin-singlet s-wave superconductor, where the pair potential is induced in the QAH (hereinafter we refer to it as QAH+s). The system is described by the BdG Hamiltonian,

$$\mathcal{H}_{\mathrm{BdG}}(\boldsymbol{k}) = d_z(\boldsymbol{k})s_z + [d_x(\boldsymbol{k})s_x + d_y(\boldsymbol{k})s_y]\tau_z - \mu\tau_z + \Delta\tau_x, \tag{2}$$

where τ_i is Pauli matrix in Nambu space, μ is the chemical potential, and Δ is the induced pair potential of spin-singlet s-wave superconductor. The energy gap of $\mathcal{H}_{\mathrm{BdG}}$ at $\boldsymbol{k} = \boldsymbol{0}$ is given by $E_{\mathrm{g}} = |m| - \sqrt{\Delta^2 + \mu^2}$. The present system has three phases, i.e. $\mathcal{N} = 0, 1$, and 2 phases,[70] which are realized in $m > \sqrt{\Delta^2 + \mu^2}$, $|m| < \sqrt{\Delta^2 + \mu^2}$, and $m < -\sqrt{\Delta^2 + \mu^2}$, respectively.

B. Surface local density of states

In order to obtain the SLDOS at the edge ($x = 1$), we introduce an infinite potential barrier at $x = 0$. We calculate the Green's function at $x = 1$ by t-matrix formulation.[82] The system is infinite along the y-direction while it is semi-infinite along the x-direction. Since translational invariance is absent along the x-direction, only the momentum k_y in the y-direction is a good quantum number. We express the Green's function in the spatial coordinates x and x' for fixed k_y as follows;

$$\begin{aligned} G_{xx'}(k_y, \omega) &= g_{xx'}(k_y, \omega) \\ &\quad - g_{x0}(k_y, \omega)g_{00}^{-1}(k_y, \omega)g_{0x'}(k_y, \omega), \end{aligned} \tag{3}$$

with

$$g_{xx'}(k_y, \omega) = \frac{1}{N_x} \sum_{k_x} e^{ik_x(x-x')} g(k_x, k_y, \omega), \tag{4}$$
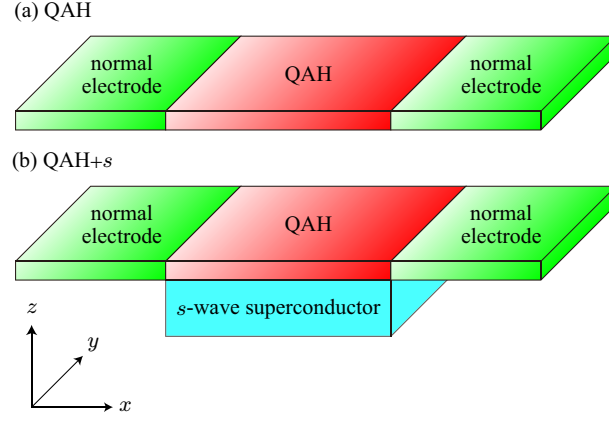
FIG. 1. (color online) Schematic illustrations of N/QAH/N (a) and N/(QAH+s)/N (b) junctions .

and

$$g^{-1}(k_x, k_y, \omega) = \omega - \mathcal{H}_{\mathrm{BdG}}(k_x, k_y), \tag{5}$$

where N_x is the total number of lattice points in the x-direction. In the right hand side of Eq.(3), the first term denotes the unperturbed bulk Green function, and the second term comes from the scattering effect at the edge. The angle resolved SLDOS $N(k_y, \omega)$ at $x = 1$ is written as

$$N(k_y, \omega) = -\frac{1}{\pi} \mathrm{Im} \mathrm{Tr} \left[P_{\mathrm{e}} G_{11}^{\mathrm{R}}(k_y, \omega) \right], \tag{6}$$

where

$$G_{xx'}^{\mathrm{R}}(k_y, \omega) = G_{xx'}(k_y, \omega + i\eta), \tag{7}$$

is the retarded Green's function, η is an infinitesimal positive number, and $P_{\mathrm{e}} = (1 + \tau_z)/2$ is the projection operator onto the particle subspace. From the above equations, one obtains the SLDOS $D(\omega)$ for energy ω measured from the Fermi level as follows

$$D(\omega) = \frac{1}{N_y} \sum_{k_y} N(k_y, \omega), \tag{8}$$

where N_y is a total number of lattice points for the y-direction. In the actual calculation, we set $N_x = N_y = 4096$.

C.   N/(QAH+s)/N junction

Now we show the Hamiltonian of N/(QAH+s)/N junction illustrated in Fig.1. The Hamiltonian of QAH+s in the center region of the junction is represented as

$$\mathcal{H}_{\mathrm{BdG}}(k_y) = \sum_{x=1}^{N_{\mathrm{QAH}}} c_x^{\dagger}(k_y) \epsilon(k_y) c_x(k_y)$$
$$+ \sum_{x=1}^{N_{\mathrm{QAH}}-1} \left[c_x^{\dagger}(k_y) t_{\mathrm{QAH}} c_{x+1}(k_y) + \mathrm{h.c.} \right], \tag{9}$$

with

$$\epsilon(k_y) = [m + 2B(2 - \cos k_y)]s_z + A \sin k_y s_y \tau_z + \Delta \tau_x, \tag{10}$$

and

$$t_{\mathrm{QAH}} = -Bs_z - iAs_x \tau_z/2. \tag{11}$$

The Hamiltonians of normal electrodes located in the left ($\mathcal{H}_L$) and the right ($\mathcal{H}_R$) regions are given by

$$\mathcal{H}_L(k_y) = \sum_{x=-\infty}^{0} c_x^\dagger(k_y)(-2t_N \cos k_y - \mu_N)\tau_z c_x(k_y)$$
$$+ \left(\sum_{x=-\infty}^{-1} c_x^\dagger(k_y)(-t_N)\tau_z c_{x+1}(k_y) + \text{h.c.} \right), \tag{12}$$

$$\mathcal{H}_R(k_y) = \sum_{x=N_{QAH}+1}^{\infty} c_x^\dagger(k_y)(-2t_N \cos k_y - \mu_N)\tau_z c_x(k_y)$$
$$+ \left(\sum_{x=N_{QAH}+1}^{\infty} c_x^\dagger(k_y)(-t_N)\tau_z c_{x+1}(k_y) + \text{h.c.} \right). \tag{13}$$

We also assume the following simple hopping $\mathcal{H}_j$ between the electrode and the QAH+s,

$$\mathcal{H}_j(k_y) = c_0^\dagger(k_y)(-t_j)\tau_z c_1(k_y)$$
$$+ c_{N_{QAH}}^\dagger(k_y)(-t_j)\tau_z c_{N_{QAH}+1}(k_y) + \text{h.c.} \tag{14}$$

In the actual calculation, t_j is fixed as $t_j = t_N$, for simplicity.

D. Tunneling conductance and recursive Green's function

The angle resolved tunneling conductance $\gamma(p_y, \omega)$ in a junction is given by the Lee-Fisher formula[83]

$$\gamma(p_y, \omega) = \frac{t_j^2 e^2}{2h}\text{Tr}\left[P_e(G_{x,x+1}'' G_{x,x+1}'' + G_{x+1,x}'' G_{x+1,x}'' \right.$$
$$\left. - G_{x,x}'' G_{x+1,x+1}'' - G_{x+1,x+1}'' G_{x,x}'')\right], \tag{15}$$

with $G_{xx'}'' = \text{Im}\, G_{xx'}^R$. Due to current conservation in the normal metals, we can choose arbitrary x for Eq.(15) in $x < 0$ or $x \geq N_{QAH} + 1$, except in the superconducting region ($1 \leq x \leq N_{QAH}$). The total conductance Γ is given by $\Gamma(\omega) = \sum_{p_y} \gamma(p_y, \omega)$. We first calculate the Green's function $G_{L,l,l}$ in the left semi-infinite system where the sites in $x > l$ are deleted. $G_{L,x,x}$ satisfies the following recursive relation:

$$G_{L,x,x}^{-1} = g_x^{-1} - \mathcal{H}_{x,x-1} G_{L,x-1,x-1} \mathcal{H}_{x-1,x}, \tag{16}$$

with $\mathcal{H}_{x,x'}$ being the hopping from x' to x. Here, $g_x^{-1}(p_y, \omega) = \omega - \mathcal{H}_{x,x}(p_y)$ is the Green's function in the isolated x-th column. In the present model, only $\mathcal{H}_{x,x'}$ with $|x - x'| \leq 1$ is nonzero, and given by

$$\mathcal{H}_{x,x'} = [(-2t_N \cos k_y - \mu_N)\delta_{x,x'} - t_N \delta_{x',x\pm1}]\tau_z, \tag{17}$$

for $x, x' \leq 0$ or $x, x' \geq N_{QAH} + 1$, and

$$\mathcal{H}_{x,x'} = \epsilon(k_y)\delta_{x,x'} + t_{QAH}\delta_{x',x+1} + t_{QAH}^\dagger \delta_{x',x-1}, \tag{18}$$

for $1 \leq x, x' \leq N_{QAH}$. At the interfaces, $\mathcal{H}_{0,1}$, $\mathcal{H}_{1,0}$, $\mathcal{H}_{N_{QAH},N_{QAH}+1}$ and $\mathcal{H}_{N_{QAH}+1,N_{QAH}}$ are given by

$$\mathcal{H}_{0,1} = \mathcal{H}_{1,0}^\dagger = \mathcal{H}_{N_{QAH},N_{QAH}+1}^\dagger = \mathcal{H}_{N_{QAH}+1,N_{QAH}}$$
$$= -t_j \tau_z. \tag{19}$$

The Green's function in the right semi-infinite system $G_{R,l,l}$ where the sites in $x < l$ are deleted satisfies the following relation.

$$G_{R,x,x}^{-1} = g_x^{-1} - \mathcal{H}_{x,x+1} G_{R,x+1,x+1} \mathcal{H}_{x+1,x}. \tag{20}$$
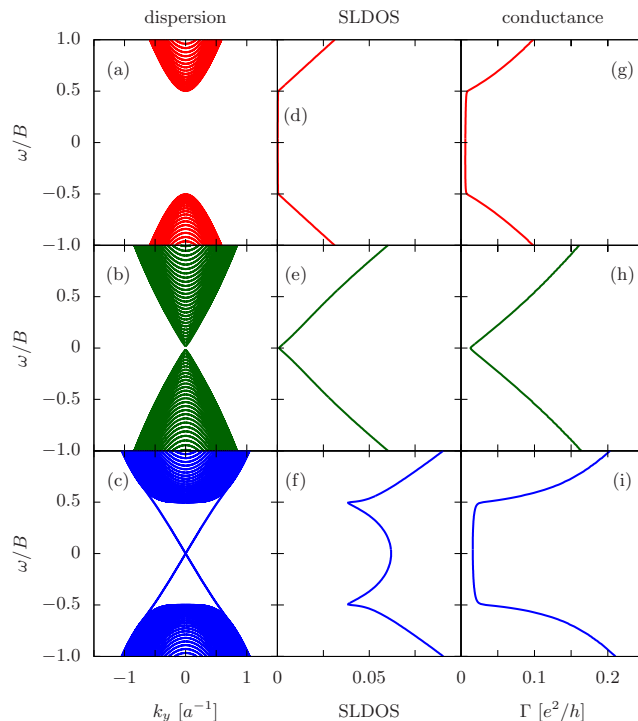
FIG. 2. (color online) Energy dispersion relations [(a),(b), and (c)], SLDOS [(d), (e), and (f)], and the tunneling conductances in N/QAH/N junction, for the case with the trivial insulator [(g):$m/B = 0.5$], the critical point [(h):$m = 0$], and the QAH [(c):$m/B = -0.5$]. a denotes the lattice constant. The parameters are taken as follows. $A/B = 1$, $\Delta = \mu = 0$, and $N_{\mathrm{QAH}} = 100$ for the energy dispersion, $N_{\mathrm{QAH}} = 4096$ for the SLDOS, $N_{\mathrm{QAH}} = 1000$ for the conductance.

It is noted that the Green's functions at the edge of the electrode ($G_{\mathrm{L},0,0}$ and $G_{\mathrm{R},N_{\mathrm{QAH}}+1,N_{\mathrm{QAH}}+1}$) are obtained by Eq.(3). Then, using Eqs. (16) and (20), we can recursively obtain $G_{\mathrm{L},x,x}$ and $G_{\mathrm{R},x,x}$ for any x. The site-diagonal part of the Green's function is obtained in terms of the above Green's functions,

$$
\begin{aligned}
G_{x,x}^{-1} = g_x^{-1} &- \mathcal{H}_{x,x-1} G_{\mathrm{L},x-1,x-1} \mathcal{H}_{x-1,x} \\
&- \mathcal{H}_{x,x+1} G_{\mathrm{R},x+1,x+1} \mathcal{H}_{x+1,x},
\end{aligned}
\tag{21}
$$

and the site-off-diagonal parts are also obtained as

$$
G_{x,x+1} = G_{x,x} \mathcal{H}_{x,x+1} G_{\mathrm{R},x+1,x+1},
\tag{22}
$$
$$
G_{x+1,x} = G_{x+1,x+1} \mathcal{H}_{x+1,x} G_{\mathrm{L},x,x}.
\tag{23}
$$

We can calculate the conductance Γ from $G_{x,x}$, $G_{x+1,x+1}$, $G_{x,x+1}$, and $G_{x+1,1}$ by using Eq. (15).

III. RESULTS AND DISCUSSIONS

In this section, we show our numerical results for the electronic states and the tunneling conductance of the QAH+s. Experimental proposals to detect our results are also discussed.

A. Electronic states and tunneling conductance in N/QAH/N junction

Before discussing the superconducting case, we check the electronic states and the tunneling conductance of the N/QAH/N junction at $\Delta = \mu = 0$. The energy dispersions with the finite width ($N_{\mathrm{QAH}} = 100$) are shown in Figs. 2(a), (b), and (c). There is a band gap in Figs. 2(a) and 2(c), respectively, while it closes at the critical point with $m = 0$ [Fig. 2(b)]. Gapless chiral edge modes show up when $m < 0$ [Fig. 2(c)]. Note that two gapless modes propagating in opposite directions appear in Fig. 2(c) since both the left ($x = 0$) and right edges ($x = N_{\mathrm{QAH}}$) are
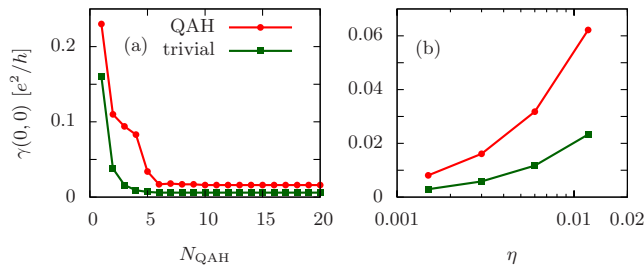
FIG. 3. (color online) Angle resolved tunneling conductance $\gamma(k_y, \omega)$ at $k_y = 0$ and $\omega = 0$ as functions of $N_{\rm QAH}$ (a) and η (b), for the QAH with $m/B = -0.5$ and the trivial insulator with $m/B = 0.5$ and $N_{\rm QAH} = 1000$. The parameters are the same as in Fig. 2.

present in the calculation, i.e., each edge has an edge state. Figures 2(d), (e), and (f) show the SLDOS at the edge. In the trivial insulator phase with $m \geq 0$ [Fig. 2(d) and (e)], the line shapes of the SLDOS are the same as those in the bulk. On the other hand, in the case of QAH, the SLDOS is enhanced in the band gap due to the gapless edge modes, as shown in Fig. 2(f).

The line shapes of tunneling conductance are similar to those of the SLDOS when $m \geq 0$ [Fig.2(g) and (h)], i.e., U-shaped gap in $|\omega| < m$ [Fig.2(g)] and V-shaped dip at $m = 0$ [Fig.2(h)]. In the case of QAH, although the SLDOS shows a zero-energy peak [Fig.2(f)], the corresponding tunneling conductance shows a U-shaped gap [Fig.2(i)] similar to that in the case with $m > 0$ [Fig. 2(g)]. This is because the central region of the junction has a bulk gap, thus the tunneling conductance should be zero.

Here we notice that the conductance in Figs. 2(g) and (i) takes a small but non-zero value in the energy gap, but this comes from a nonzero value of η in our numerical calculation. Indeed, as one decreases η in Eq. (7) and increases the number of QAH layer ($N_{\rm QAH}$), $\gamma(0,0)$ tends to be zero, as shown in Fig. 3, i.e., the corresponding conductance goes to zero in the limit of $N_{\rm QAH} \to \infty$ and $\eta \to +0$. Additionally, we note that the tunneling conductance of the QAH is lager than that of the trivial insulator for finite $N_{\rm QAH}$ and η (Fig.3). This is due to hybridization of the edge states located at $x = 0$ and $x = N_{\rm QAH}$.

B. Electronic states of QAH+s

Now we consider the superconducting case with $\Delta/B = 0.25$. The trivial superconductor with $\mathcal{N} = 0$ does not have any gapless state as shown in Fig. 4(a), while the topological superconductors with $\mathcal{N} = 1$ [Fig.4(b)] and $\mathcal{N} = 2$ [Fig.4(c)] have. Although the gapless modes in the latter two phases have a similar energy dispersion, we can distinguish them by the SLDOS, as shown in Figs. 4(e) and (f): The line shape of the SLDOS for $\mathcal{N} = 1$ shows a zero-bias peak [Fig.4(e)]. On the other hand, that for $\mathcal{N} = 2$ shows a larger zero-bias peak and satellite peaks at $\omega/E_{\rm g} \sim \pm 2$ [Fig. 4(f)]. The larger zero-bias peak is due to two gapless modes, and the satellite peaks come from a branch of ABS near the bulk bands.

C. Even-odd effect in the angle resolved conductance

Next we discuss the angle resolved conductance $\gamma(k_y, \omega)$ in the N/(QAH+s)/N junction shown in Fig. 5. In $\mathcal{N} = 0$ [Fig. 5(a)] and $\mathcal{N} = 1$ [Fig. 5(b)] phases, the conductance spectra are naturally understood by the energy spectra [Figs. 4(a)(b)] and the SLDOSs [Figs. 4(d)(e)]. Due to resonance between the incident state and the chiral edge mode, the value of conductance in $\mathcal{N} = 1$ phase takes $\gamma(k_y, \omega) \sim 2e^2/h$ at $\omega = E_{\rm edge}(k_y)$, where $E_{\rm edge}(k_y)$ is the energy dispersion relation of the edge state. Note that the conductance spectra are asymmetric with respect to $k_y = 0$ because the present edge mode is *chiral*.

In $\mathcal{N} = 2$ phase, we obtain a remarkable result: In this phase, it is natively expected that the tunneling conductance take a doubled value of that in $\mathcal{N} = 1$ phase since there are two edge modes. It is, however, not the case. As shown in Fig. 5(c), in $\mathcal{N} = 2$ phase, the conductance takes a *smaller* value than that in $\mathcal{N} = 1$ phase at $\omega \sim E_{\rm edge}(k_y)$. In particular, the conductance vanishes just at $\omega = E_{\rm edge}(k_y)$. To confirm this, we study $\gamma(k_y, \omega)$ at $k_y = 0$ and $\omega = 0$ as functions of $N_{\rm QAH}$ [Fig. 6(a)] and η [Fig. 6(b)]. It is found that as $N_{\rm QAH}$ increases and η decreases, $\gamma(0,0)$ converges to $2e^2/h$ in $\mathcal{N} = 1$ phase, and to 0 in $\mathcal{N} = 0, 2$ phases. Therefore, the conductance shows an *even-odd effect* as $\gamma = [1 - (-1)^{\mathcal{N}}]e^2/h$ in the presence of chiral Majorana fermions.
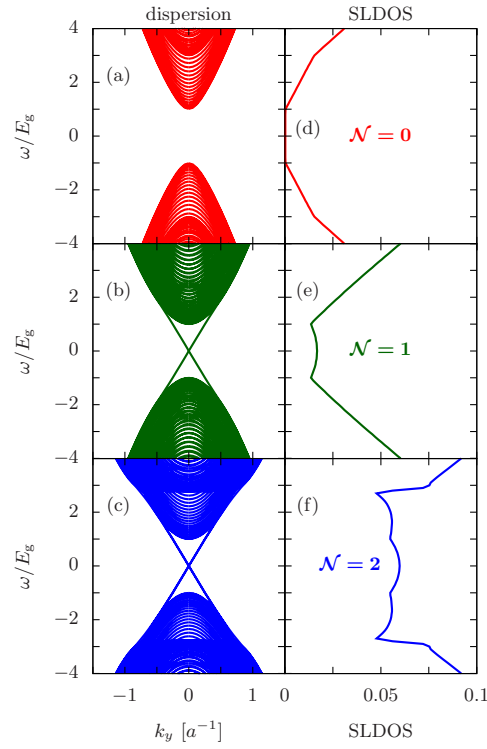
FIG. 4. (color online) Energy dispersion relations and the SLDOSs in QAH+s with $\mathcal{N} = 0$ [(a) and (d): $m/B = 0.5$], $\mathcal{N} = 1$ [(b) and (e): $m = 0$], and $\mathcal{N} = 2$ [(c) and (f): $m/B = -0.5$]. The pair potential is taken to be $\Delta/B = 0.25$, and the other parameters are the same as in Fig. 2.
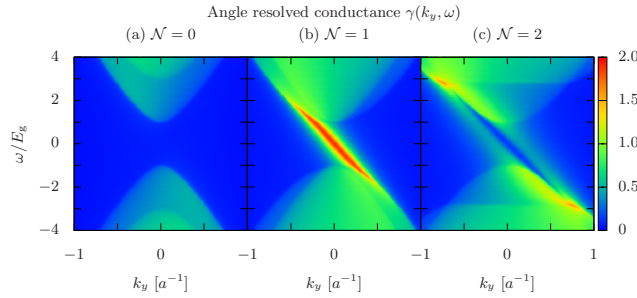
FIG. 5. (color online) Angle resolved conductance in N/(QAH+s)/N junction with $\mathcal{N} = 0$ (a), $\mathcal{N} = 1$ (b), and $\mathcal{N} = 2$ (c) phases.
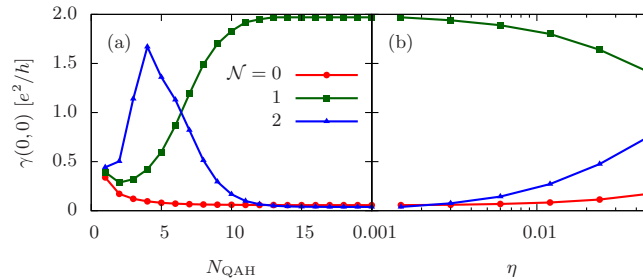
FIG. 6. (color online) Angle resolved conductance γ at $k_y = 0$ and $\omega = 0$ as functions of N_{QAH} (a) and η (b).
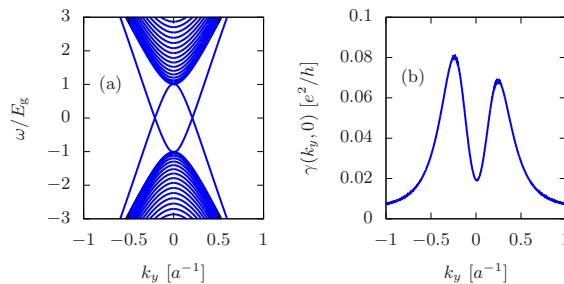
FIG. 7. (color online) The energy dispersion of the QAH+s (a) and the angle resolved conductances (b) in $\mathcal{N} = 2$ phase. The chemical potentials are set to be $\mu/B = 0.3$. The energy gap is given by $E_{\mathrm{g}}/B = 0.11$.

The vanishment of the tunneling conductance originates from the degeneracy of Majorana edge fermions in $\mathcal{N} = 2$ phase: Indeed, it is suppressed by lifting the degeneracy by tuning the chemical potential or applying Zeeman fields. At a finite chemical potential, the degeneracy of the gapless modes is lifted and the zero energy states appear at the two finite k_y points, as shown in Fig. 7(a). The conductance at $\omega = 0$ with the finite μ is shown in Fig. 7(b). Contrary to that with $\mu = 0$, $\gamma(0,0)$ remains non-zero. This result suggests that the vanished conductance arises from interference of degenerated Majorana fermions.

Here we note that the degeneracy of Majorana edge fermions is ensured by a symmetry of the system: When $\mu = 0$, the BdG Hamiltonian (2) has the following additional symmetry,

$$s_y \tau_z \mathcal{H}_{\mathrm{BdG}}(k_x, k_y) s_y \tau_z = -\mathcal{H}_{\mathrm{BdG}}(k_x, -k_y), \tag{24}$$

and on the k_x axis, this reduces to the so called chiral symmetry,

$$\{\Gamma, \mathcal{H}_{\mathrm{BdG}}(k_x, 0)\} = 0, \tag{25}$$

with $\Gamma = s_y \tau_z$. Thus, following Refs.17 and 35, one can introduce the one-dimensional winding number,

$$W = -\frac{1}{4\pi i} \int_{-\pi}^{\pi} dk_x \mathrm{tr} \left[\Gamma \mathcal{H}_{\mathrm{BdG}}^{-1} \partial_{k_x} \mathcal{H}_{\mathrm{BdG}} \right]_{k_y = 0}, \tag{26}$$

which can be evaluated as $W = 2$ in the case of $\mathcal{N} = 2$.[72] Therefore, the bulk-edge correspondence ensures that there exist two degenerate Majorana edge modes at $k_y = 0$. As we mentioned above, because the vanishment of the tunneling conductance occurs only when Majorana edge modes are degenerate, it is very likely that this chiral symmetry is responsible for the destructive interference of the tunneling conductance reported here.

In the normal (not superconducting) states, even-odd effects in conductance appear in mono/bi-layer graphene,[84] which can be generalized to the system with spin-orbit interactions.[85] They are interpreted as a result of mirror symmetry of the system.[86] Also, graphene nano-ribbons show even-odd effects in the conductance[87–89], which can be understood using parity of the system. We believe that our result is also explained in the viewpoint of symmetry.

On the other hand, in superconducting states, various even-odd effects of Majorana fermions have been reported so far. For instance, in N / a chain of Majorana bound states junction, the tunneling conductance shows an even-odd effect as a function of the length of the chain.[90] It has been also known that the SLDOS at the zero energy in a multiband Rashba superconductor with Zeeman interaction shows an even-odd effect as a function of the number of occupied subband.[91] In these cases, no degeneracy of Majorana fermion exists by hybridization when the number of the Majorana fermions is even. On the other hand, in our case, the degeneracy in $\mathcal{N} = 2$ phase is essential to obtain the even-odd effects. Therefore, the even-odd effect reported in the present paper is essentially distinct from the previous ones, and it originates from the interference without using interferometers as discussed in Refs. 58, 59, and 92

D. Proposals for experiment

Before closing the section, we propose how to detect the even-odd effect mentioned above. The simplest observable is the angle-integrated tunneling conductance. In $\mathcal{N} = 0$ phase, the system has no gapless mode, then the value of conductance becomes smaller in the energy gap, as shown in Fig. 8 (red line). In $\mathcal{N} = 1$ phase, the line shape of conductance shows a zero-bias peak due to gapless mode [Fig. 8 (green line)]. On the other hand, in $\mathcal{N} = 2$ phase, the line shape of conductance shows a zero-bias dip [Fig. 8 (blue line)], in spite of the presence of gapless modes.
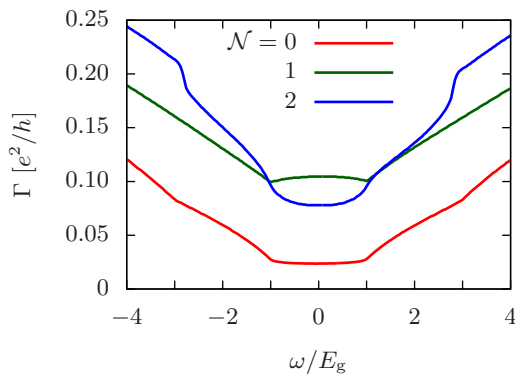
FIG. 8. (color online) Tunneling conductances in the N/(QAH+s)/N junction with $\mathcal{N} = 0$, $\mathcal{N} = 1$, and $\mathcal{N} = 2$ phases.

The more direct evidence is to observe the angle resolved current by scanning a charged tip above the system as was performed for two-dimensional electron gases in GaAs heterostructures.[93,94] Moreover, it is useful to fabricate the nanoribbon of N/(QAH+s)/N junction since normal incident electron with $k_y = 0$ effectively contributes to $\gamma(0,0)$.

IV. SUMMARY

We studied the tunneling conductances of N/(QAH+s)/N junction in $\mathcal{N} = 0$, $\mathcal{N} = 1$, and $\mathcal{N} = 2$ phases. In the presence of gapless edge modes in $\mathcal{N} = 1$ and $\mathcal{N} = 2$ phases, the corresponding SLDOSs take finite values in the bulk energy gap. In $\mathcal{N} = 1$ phase the angle resolved conductance also takes the finite value of $\gamma(k_y, \omega) = 2e^2/h$ when the incident electron is resonant with the chiral edge mode at $\omega = E_{\text{edge}}(k_y)$. On the contrary, in $\mathcal{N} = 2$ phase, the tunneling conductance vanishes at $\omega = E_{\text{edge}}(k_y)$ although the corresponding SLDOS does not. This stems from the interference of the degenerated Majorana fermions. Namely, an even-odd effect with respect to the number of Majorana fermion $\mathcal{N}$ occurs.

Although we have partly addressed the mechanism of the even-odd effect, it has been not definitely answered. To reveal this, the following things are needed to be unveiled: relation between the chiral symmetry and the tunneling conductance, robustness of the even-odd effect against disorder proved by the microscopic calculation, and the even-odd effect for the higher Chern number of $\mathcal{N} \geq 3$. We will study these issues in the future work.

ACKNOWLEDGMENTS

Appendix A: Tunneling conductance of N/(QAH+s) junction in the continuum limit

To confirm the even-odd effect found in this paper, we study the tunneling conductance of N/(QAH+s) junction in the continuum limit.

Let us consider a normal metal in the left side ($x < 0$), whose Hamiltonian is given by

$$H_{\text{N}}(\boldsymbol{k}) = \left(\frac{k^2}{2m_{\text{e}}} - \mu_{\text{N}} \right) \tau_z, \tag{A1}$$

and QAH+s in the right side ($x > 0$). Here $k = (k_x^2 + k_y^2)^{1/2}$ is the magnitude of the two-dimensional momentum. The Hamiltonian of QAH+s is obtained by the $k \cdot p$ theory as[70]

$$H(\boldsymbol{k}) = m(\boldsymbol{k})s_z + Aa(k_x s_x + k_y s_y)\tau_z - \mu\tau_z + \Delta\tau_x, \tag{A2}$$

$$m(\boldsymbol{k}) = m + B(ka)^2. \tag{A3}$$
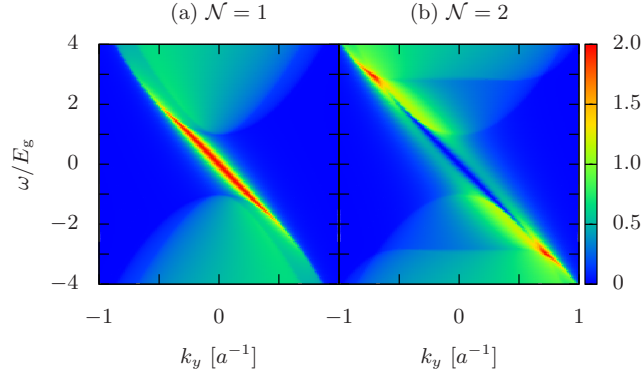
FIG. 9. (color online) Angle resolved conductance $\gamma(k_y, \omega)$ of the N/(QAH+s) junction for $\mathcal{N} = 1$ with $\tilde{\mu} = \mu/B = 0$ (a) and $\mathcal{N} = 2$ with $\tilde{\mu} = 0.3$ (b) phases. $E_{\mathrm{g}} = 0.25B$ is the magnitude of the superconducting gap.

The eigenvalue of the above Hamiltonian is given by

$$E_{\alpha\beta}(\boldsymbol{k}) = \alpha\Big[m^2(\boldsymbol{k}) + A^2 k^2 a^2 + \mu^2 + \Delta^2 +$$
$$+ 2\beta\sqrt{(m^2(\boldsymbol{k}) + A^2 k^2 a^2)\mu^2 + m^2(\boldsymbol{k})\Delta^2}\Big], \tag{A4}$$

where $\alpha, \beta = \pm$. The corresponding eigenvector $\boldsymbol{u}_{\alpha\beta}(\boldsymbol{k})$ is also obtained analytically.

Now we calculate the tunneling conductance, generalizing theories of the tunneling spectroscopy of conventional[95] and unconventional[6,96] superconductors. The wave function in the normal metal ($x < 0$) is given by

$$\psi_{\mathrm{N},s}(\boldsymbol{x}) = \Big[\chi_{se}e^{ik_{\mathrm{ex}}x} + \sum_{s'}\big(b_{ss'}\chi_{s'e}e^{-ik_{\mathrm{ex}}x}$$
$$+ a_{ss'}\chi_{s'\mathrm{h}}e^{ik_{\mathrm{hx}}x}\big)\Big]e^{ik_y y}, \tag{A5}$$

where $\chi_{s\tau}$ is the eigenvector of $H_{\mathrm{N}}(\boldsymbol{k})$ with spin s for electron ($\tau = \mathrm{e}$) or hole ($\tau = \mathrm{h}$), and $k_{\mathrm{ex}} = (k_{\mathrm{e}}^2 - k_y^2)^{1/2} = k_{\mathrm{e}}\cos\theta$, $k_{\mathrm{e}} = \sqrt{2m_{\mathrm{e}}(\mu_{\mathrm{N}} + E)}$, $k_{\mathrm{hx}} = [2m_{\mathrm{e}}(\mu_{\mathrm{N}} - E) - k_y^2]^{1/2}$. The first term of the wave function denotes an injected electron, and the second (third) one denotes a reflected hole (electron) with reflection coefficient $a_{ss'}$ ($b_{ss'}$). The wave function in the QAH+s ($x > 0$) is given by

$$\psi_{\mathrm{QAH}+s}(x) = \sum_i t_i \boldsymbol{u}_i e^{i(q_i x + k_y y)}, \tag{A6}$$

where q_i, ($i = 1, \cdots, 4$) is a solution of $E = E_{\alpha_i\beta_i}(q_i, k_y)$. Among the eigenvectors, $\psi_{\mathrm{QAH}+s}(\boldsymbol{x})$ consists of those with $E_{\alpha_i\beta_i}(q_i, k_y)/\partial q_i > 0$ or $\mathrm{Im}(q_i) > 0$, where the former denotes right-going states and the latter denotes localized states in the vicinity of $x = 0$. These wave functions are connected at the interface ($x = 0$) by the conditions[97], $\psi_{\mathrm{N}}(0) = \psi_{\mathrm{QAH}+s}(0)$ and $v_{\mathrm{N}}\psi_{\mathrm{N}}(0) = v_{\mathrm{QAH}+s}\psi_{\mathrm{QAH}+s}(0)$, with the velocity operator $v_{\mathrm{N(QAH}+s)} = \partial H_{\mathrm{N(QAH}+s)}/\partial k_x|_{k_x \to -i\partial_x}$. The above equations determine the coefficients $a_{ss'}$, $b_{ss'}$ and t_i. Finally, the charge conductance $\gamma(k_y, \omega)$ is given by

$$\gamma(k_y, \omega) = \frac{e^2}{h}\left[2 + \sum_{ss'}\big(|a_{ss'}|^2 - |b_{ss'}|^2\big)\right]. \tag{A7}$$

In the following, the material parameters of the normal metal are fixed as $m_{\mathrm{e}}Ba^2 = 1$, $\mu_{\mathrm{N}}/B = 100$, and the material parameters of QAH+s are chosen as $A = B$ and $\Delta/B = 0.25$.

The obtained angle resolved tunneling conductances are shown in Fig. 9. These spectra are consistent with those obtained in the lattice model shown in Fig. 5; the value of $\gamma(k_y, E_{\mathrm{edge}}(k_y))$ takes $2e^2/h$ in $\mathcal{N} = 1$ phase [Fig. 9(a)] while it takes 0 in $\mathcal{N} = 2$ phase [Fig. 9(b)]. In order to see the even-odd effect more clearly, we focus on $\gamma(k_y, 0)$. Figure 10(a) shows the angle resolved conductance at the zero-bias voltage ($\omega = 0$), where the branch of Majorana fermions appears at $k_y = 0$, i.e., $E_{\mathrm{edge}}(0) = 0$, both for $\mathcal{N} = 1$ and $\mathcal{N} = 2$ phases. The value of $\gamma(0, 0)$ takes $2e^2/h$ in $\mathcal{N} = 1$ phase and 0 in $\mathcal{N} = 2$ phase. However, if one tunes the chemical potential μ away from zero, where the degeneracy of two Majorana fermions is lifted, the value of conductance recovers to be finite at $k_y = 0$, as shown in Fig. 10(b).
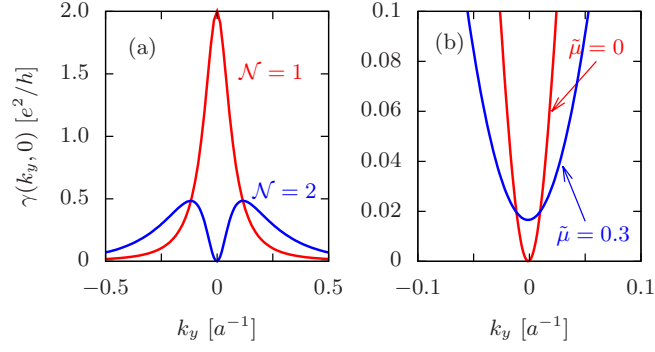
FIG. 10. (color online) The angle resolved tunneling conductance $\gamma(k_y, 0)$ at the zero-bias voltage $\omega = 0$ for $\mathcal{N} = 1$ and $\mathcal{N} = 2$ phases (a). Those in $\mathcal{N} = 2$ phase for $\tilde{\mu} = \mu/B = 0$ and $\tilde{\mu} = 0.3$ are also shown (b).

As compared to the calculation in the lattice system, the present approach in the appendix has advantages, i.e., it is easy to take the thermodynamic limit, and the infinitesimal small factor η is not necessary. The above result indicates that the even-odd effect found in this paper is robust, and the vanishing conductance is driven by the degenerating two Majorana fermions.

[1] L. J. Buchholtz and G. Zwicknagl, Phys. Rev. B **23**, 5788 (1981).

[2] J. Hara and K. Nagai, Prog. Theor. Phys. **76**, 1237 (1986).

[3] S. Kashiwaya and Y. Tanaka, Reports on Progress in Physics **63**, 1641 (2000).

[4] T. Löfwander, V. S. Shumeiko, and G. Wendin, Superconductor Science and Technology **14**, R53 (2001).

[5] C.-R. Hu, Phys. Rev. Lett. **72**, 1526 (1994).

[6] Y. Tanaka and S. Kashiwaya, Phys. Rev. Lett. **74**, 3451 (1995).

[7] Y. Tanaka and S. Kashiwaya, Phys. Rev. B **53**, 9371 (1996).

[8] Y. Asano, Y. Tanaka, and S. Kashiwaya, Phys. Rev. B **69**, 134501 (2004).

[9] X.-L. Qi, T. L. Hughes, S. Raghu, and S.-C. Zhang, Phys. Rev. Lett. **102**, 187001 (2009).

[10] R. Roy, cond-mat/0608064.

[11] M. Sato, Phys. Rev. B **79**, 214526 (2009).

[12] M. Sato, Phys. Rev. B **81**, 220504 (2010).

[13] A. P. Schnyder, S. Ryu, A. Furusaki, and A. W. W. Ludwig, Phys. Rev. B **78**, 195125 (2008).

[14] S. Ryu, A. P. Schnyder, A. Furusaki, and A. W. W. Ludwig, New Journal of Physics **12**, 065010 (2010).

[15] J. C. Y. Teo and C. L. Kane, Phys. Rev. B **82**, 115120 (2010).

[16] Y. Tanaka, M. Sato, and N. Nagaosa, J. Phys. Soc. Jpn. **81**, 011013 (2012).

[17] M. Sato, Y. Tanaka, K. Yada, and T. Yokoyama, Phys. Rev. B **83**, 224511 (2011).

[18] K. Yada, M. Sato, Y. Tanaka, and T. Yokoyama, Phys. Rev. B **83**, 064505 (2011).

[19] M. Matsumoto and M. Sigrist, J. Phys. Soc. Jpn. **68**, 994 (1999).

[20] C. Honerkamp and M. Sigristt, J. Low Temp. Phys. **111**, 895 (1998), 10.1023/A:1022281409397.

[21] M. Yamashiro, Y. Tanaka, and S. Kashiwaya, Phys. Rev. B **56**, 7847 (1997).

[22] A. Furusaki, M. Matsumoto, and M. Sigrist, Phys. Rev. B **64**, 054514 (2001).

[23] Y. Maeno, H. Hashimoto, K. Yoshida, S. Nishizaki, T. Fujita, J. Bednorz, and F. Lichtenberg, Nature **372**, 532 (1994).

[24] S. Kashiwaya, H. Kashiwaya, H. Kambara, T. Furuta, H. Yaguchi, Y. Tanaka, and Y. Maeno, Phys. Rev. Lett. **107**, 077003 (2011).

[25] D. J. Thouless, M. Kohmoto, M. P. Nightingale, and M. den Nijs, Phys. Rev. Lett. **49**, 405 (1982).

[26] M. Kohmoto, Ann. Phys. **160**, 343 (1985).

[27] M. Z. Hasan and C. L. Kane, Rev. Mod. Phys. **82**, 3045 (2010).

[28] E. Bauer, G. Hilscher, H. Michor, C. Paul, E. W. Scheidt, A. Gribanov, Y. Seropegin, H. Noël, M. Sigrist, and P. Rogl, Phys. Rev. Lett. **92**, 027003 (2004).

[29] K. Togano, P. Badica, Y. Nakamori, S. Orimo, H. Takeya, and K. Hirata, Phys. Rev. Lett. **93**, 247004 (2004).

[30] M. Nishiyama, Y. Inada, and G.-q. Zheng, Phys. Rev. B **71**, 220505 (2005).

[31] A. D. Hillier, J. Quintanilla, and R. Cywinski, Phys. Rev. Lett. **102**, 117007 (2009).

[32] N. Reyren, S. Thiel, A. Caviglia, L. Kourkoutis, G. Hammerl, C. Richter, C. Schneider, T. Kopp, A. Rüetschi, D. Jaccard, *et al.*, Science **317**, 1196 (2007).

[33] S. Nakosai, Y. Tanaka, and N. Nagaosa, Phys. Rev. Lett. **108**, 147003 (2012).

[34] M. Sato, Phys. Rev. B **73**, 214502 (2006).

[35] M. Sato and S. Fujimoto, Phys. Rev. B **79**, 094504 (2009).

[36] Y. Tanaka, T. Yokoyama, A. V. Balatsky, and N. Nagaosa, Phys. Rev. B **79**, 060505 (2009).

[37] C. Iniotakis, N. Hayashi, Y. Sawa, T. Yokoyama, U. May, Y. Tanaka, and M. Sigrist, Phys. Rev. B **76**, 012501 (2007).

[38] A. B. Vorontsov, I. Vekhter, and M. Eschrig, Phys. Rev. Lett. **101**, 127003 (2008).

[39] M. Eschrig, C. Iniotakis, and Y. Tanaka, arXiv:1001.2486.

[40] C.-K. Lu and S. Yip, Phys. Rev. B **80**, 024504 (2009).

[41] T. Yokoyama, Y. Tanaka, and J. Inoue, Phys. Rev. B **72**, 220504 (2005).

[42] A. P. Schnyder, P. M. R. Brydon, D. Manske, and C. Timm, Phys. Rev. B **82**, 184508 (2010).

[43] A. P. Schnyder and S. Ryu, Phys. Rev. B **84**, 060504 (2011).

[44] A. P. Schnyder, P. M. R. Brydon, and C. Timm, Phys. Rev. B **85**, 024522 (2012).

[45] Y. Nagato, S. Higashitani, and K. Nagai, J. Phys. Soc. Jpn. **78**, 123603 (2009).

[46] G. Volovik, JETP Lett. **90**, 587 (2009).

[47] G. Volovik, JETP Lett. **90**, 398 (2009).

[48] Y. Tsutsumi, M. Ichioka, and K. Machida, Phys. Rev. B **83**, 094510 (2011).

[49] L. Hao and T. K. Lee, Phys. Rev. B **83**, 134516 (2011).

[50] L. Fu and E. Berg, Phys. Rev. Lett. **105**, 097001 (2010).

[51] Y. S. Hor, A. J. Williams, J. G. Checkelsky, P. Roushan, J. Seo, Q. Xu, H. W. Zandbergen, A. Yazdani, N. P. Ong, and R. J. Cava, Phys. Rev. Lett. **104**, 057001 (2010).

[52] S. Sasaki, M. Kriener, K. Segawa, K. Yada, Y. Tanaka, M. Sato, and Y. Ando, Phys. Rev. Lett. **107**, 217001 (2011).

[53] M. Sato, Phys. Lett. B **575**, 126 (2003).

[54] A. Kitaev, Ann. Phys. **303**, 2 (2003).

[55] M. Freedman, A. Kitaev, M. Larsen, and Z. Wang, Bull. Amer. Math. Soc. **40**, 31 (2003).

[56] C. Nayak, S. H. Simon, A. Stern, M. Freedman, and S. Das Sarma, Rev. Mod. Phys. **80**, 1083 (2008).

[57] L. Fu and C. L. Kane, Phys. Rev. Lett. **100**, 096407 (2008).

[58] L. Fu and C. L. Kane, Phys. Rev. Lett. **102**, 216403 (2009).

[59] A. R. Akhmerov, J. Nilsson, and C. W. J. Beenakker, Phys. Rev. Lett. **102**, 216404 (2009).

[60] K. T. Law, P. A. Lee, and T. K. Ng, Phys. Rev. Lett. **103**, 237001 (2009).

[61] Y. Tanaka, T. Yokoyama, and N. Nagaosa, Phys. Rev. Lett. **103**, 107002 (2009).

[62] J. Linder, Y. Tanaka, T. Yokoyama, A. Sudbo, and N. Nagaosa, Phys. Rev. Lett. **104**, 067001 (2010).

[63] M. Sato, Y. Takahashi, and S. Fujimoto, Phys. Rev. Lett. **103**, 020401 (2009).

[64] M. Sato, Y. Takahashi, and S. Fujimoto, Phys. Rev. B **82**, 134521 (2010).

[65] J. D. Sau, R. M. Lutchyn, S. Tewari, and S. Das Sarma, Phys. Rev. Lett. **104**, 040502 (2010).

[66] J. Alicea, Phys. Rev. B **81**, 125318 (2010).

[67] R. M. Lutchyn, J. D. Sau, and S. Das Sarma, Phys. Rev. Lett. **105**, 077001 (2010).

[68] R. M. Lutchyn, T. D. Stanescu, and S. Das Sarma, Phys. Rev. Lett. **106**, 127001 (2011).

[69] Y. Oreg, G. Refael, and F. von Oppen, Phys. Rev. Lett. **105**, 177002 (2010).

[70] X.-L. Qi, T. L. Hughes, and S.-C. Zhang, Phys. Rev. B **82**, 184516 (2010).

[71] C.-X. Liu, X.-L. Qi, X. Dai, Z. Fang, and S.-C. Zhang, Phys. Rev. Lett. **101**, 146802 (2008).

[72] A. Ii, K. Yada, M. Sato, and Y. Tanaka, Phys. Rev. B **83**, 224524 (2011).

[73] S. Kashiwaya, Y. Tanaka, M. Koyanagi, and K. Kajimura, Phys. Rev. B **53**, 2667 (1996).

[74] Y. Tanaka and S. Kashiwaya, Phys. Rev. B **53**, 9371 (1996).

[75] C. Honerkamp and M. Sigrist, J. Low Temp. Phys. **111**, 895 (1998).

[76] M. Yamashiro, Y. Tanaka, and S. Kashiwaya, Phys. Rev. B **56**, 7847 (1997).

[77] M. Matsumoto and M. Sigrist, J. Phys. Soc. Jpn. **68**, 994 (1999).

[78] Y. Asano, Y. Tanaka, Y. Matsuda, and S. Kashiwaya, Phys. Rev. B **68**, 184506 (2003).

[79] T. H. Hsieh and L. Fu, Phys. Rev. Lett. **108**, 107005 (2012).

[80] A. Yamakage, K. Yada, M. Sato, and Y. Tanaka, Phys. Rev. B **85**, 180509 (2012).

[81] S. B. Chung, X.-L. Qi, J. Maciejko, and S.-C. Zhang, Phys. Rev. B **83**, 100512 (2011).

[82] M. Matsumoto and H. Shiba, J. Phys. Soc. Jpn. **64**, 1703 (1995).

[83] P. A. Lee and D. S. Fisher, Phys. Rev. Lett. **47**, 882 (1981).

[84] M. I. Katsnelson, K. S. Novoselov, and A. K. Geim, Nature Physics **2**, 620 (2006).

[85] A. Yamakage, K.-I. Imura, J. Cayssol, and Y. Kuramoto, Europhys. Lett. **87**, 47005 (2009).

[86] A. Yamakage, K.-I. Imura, J. Cayssol, and Y. Kuramoto, Phys. Rev. B **83**, 125401 (2011).

[87] A. R. Akhmerov, J. H. Bardarson, A. Rycerz, and C. W. J. Beenakker, Phys. Rev. B **77**, 205416 (2008).

[88] A. Cresti, G. Grosso, and G. P. Parravicini, Phys. Rev. B **77**, 233402 (2008).

[89] J. Nakabayashi, D. Yamamoto, and S. Kurihara, Phys. Rev. Lett. **102**, 066803 (2009).

[90] K. Flensberg, Phys. Rev. B **82**, 180516(R) (2010).

[91] A. C. Potter and P. A. Lee, Phys. Rev. B **83**, 094525 (2011).

[92] J. D. Sau, S. Tewari, and S. Das Sarma, Phys. Rev. B **84**, 085109 (2011).

[93] M. A. Topinka, B. J. LeRoy, S. E. J. Shaw, E. J. Heller, R. M. Westervelt, K. D. Maranowski, and A. C. Gossard, Science **289**, 2323 (2000).

[94] M. A. Topinka, B. J. LeRoy, R. M. Westervelt, S. E. J. Shaw, R. Fleischmann, E. J. Heller, K. D. Maranowski, and A. C. Gossard, Nature (London) **410**, 183 (2001).

[95] G. E. Blonder, M. Tinkham, and T. M. Klapwijk, Phys. Rev. B **25**, 4515 (1982).

[96] S. Kashiwaya and Y. Tanaka, Rep. Prg. Phys. **63**, 1641 (2000).

[97] L. W. Molenkamp, G. Schmidt, and G. E. W. Bauer, Phys. Rev. B **64**, 121202 (2001).